Applied Surface Science 458 (2018) 264–268

Contents lists available at ScienceDirect

Applied Surface Science

journal homepage: www.elsevier.com/locate/apsusc

# 2D Wigner crystals on silicon surface induced by nanosecond pulsed laser

Zhong-Mei Huang[c,a], Wei-Qi Huang[a,*], Shi-Rong Liu[b]

[a] Institute of Nanophotonic Physics, Guizhou University, Guiyang 550025, China
[b] State Key Laboratory of Environment Geochemistry, Institute of Geochemistry, Chinese Academy of Sciences, Guiyang 550003, China
[c] Surface Physics Laboratory, Department of Physics, Fudan University, Shanghai 200433, China

ARTICLE INFO

*Keywords:*
2D electron crystals
Two-dimensional lattices
Reflection Talbot effect
Plasma
PN junction

ABSTRACT

During pulsed laser interaction on silicon surface, the transient electron lattices occur on plasma resonance induced from faster photons on surface in our experiment. Here, it is interesting that the electron crystals can be built on plasma surface induced by intensive faster photons on silicon, which is similar with Wigner crystal in intensive electric field or intensive magnetic field. In the two-dimensional (2D) Bravais lattices, the electron crystals of three-fold, four-fold and six-fold symmetry lattices can be observed on plasma surface by using the reflecting Talbot effect images. On these surface period lattices, the decay spectrum of faster emission on the 2D transient electron crystal was measured, which is related to the faster decay peak with lifetime of 100 ns. These new phenomena have a good application in preparing the PN junction of photo-electronic devices, where the surface electron gas on plasma surface can inject into the top layer to build N type region, and the positive ions under plasma can inject into the bottom layer for forming P type region on silicon with defects in vacuum.

The physics concept of Wigner crystals was originally proposed in 1934, in which the possibility that a system of electrons in the presence of a compensating background of positive charge could crystallizes was first pointed out by Wigner [1]. Then a considerable body of work has been created devoted to the property of the three-dimensional Wigner crystal [2,3]. It has been proposed by Crandall and Williams that a two-dimensional electron crystal can be created by the application of a strong electric field perpendicular to the free surface of liquid helium, where the charge carriers can crystallize into a two-dimensional crystal in a strong electric field at low temperatures [4]. Chaplik applied this idea to electrons or holes in inversion layers near the surface of a semiconductor [5], in which the frequency spectrum calculation has been carried out [6,7]. From the above results, the plasmon dispersion relation can be obtained for a two- dimensional electron gas embedded in a three-dimensional dielectric [8]. In recent theoretical works, the role of the disorder with an elastic structure on the lattices was studied [9,10], where the important characteristic length scales, i.e., the correlation length or domain size (denoted as the Larkin length [11,12]) of the crystalline order were identified. It is interesting that some evidence of the pinning mode was obtained by a microwave experiment, in which a domain size of 100–200 nm was calculated [13]. Recent investigation has demonstrated that in 2D electron systems, the Wigner crystals and the fractional quantum Hall effect liquids are competing ground states under low temperatures and high magnetic fields [14,15].

In the article, it is discovered that the electron crystal can be built on silicon surface in an intensive photons field, as well as doing that in the strong electric field and the strong magnetic field, where it is called as the transient electron crystal. In our experiment, the nanosecond pulsed laser irradiates on silicon surface to produce plasma, in which the images of the transient electron crystals with one or two dimensional lattices on plasma surface were observed by using reflecting Talbot effect. In the two-dimensional (2D) Bravais lattices, the electron crystals of three-fold, four-fold and six-fold symmetry lattices in micrometer scale were found in the reflecting Talbot images. It is interesting to make comparison between the electron crystal lattices occurring in vacuum ($10^{-5}$Pa) and the plasmonic lattices occurring in oxygen environment of 100 Pa, in which the transient electron crystal relates to the faster decay peak with lifetime of 100 ns and the plasmonic lattice with silicon ions resonance relates to the slower decay peak with lifetime of 10 μs. It is interesting to make a comparison between the two-dimensional lattices in 2D electron crystals and the previous works such as the two pair electromagnetically induced atomic gratings [16], the two dimensional atomic lattices [17], and the optically induced atomic lattices in atomic media [18].

In plasma resonance, the plasma frequency is described by the formula: $\omega_p^2 = Ne^2/m\varepsilon$, where N is electron density and ε is the dielectric constant of the medium [19]. In a three-dimensional (3D) plasma system, the plasmon frequency is $\omega_q^2 = \omega_p^2 + (3/5)q^2$ ($hk_f$/

* Corresponding author.
*E-mail address:* wqhuang@gzu.edu.cn (W.-Q. Huang).

https://doi.org/10.1016/j.apsusc.2018.07.108
Received 25 May 2018; Received in revised form 9 July 2018; Accepted 14 July 2018
Available online 17 July 2018
0169-4332/ © 2018 Published by Elsevier B.V.

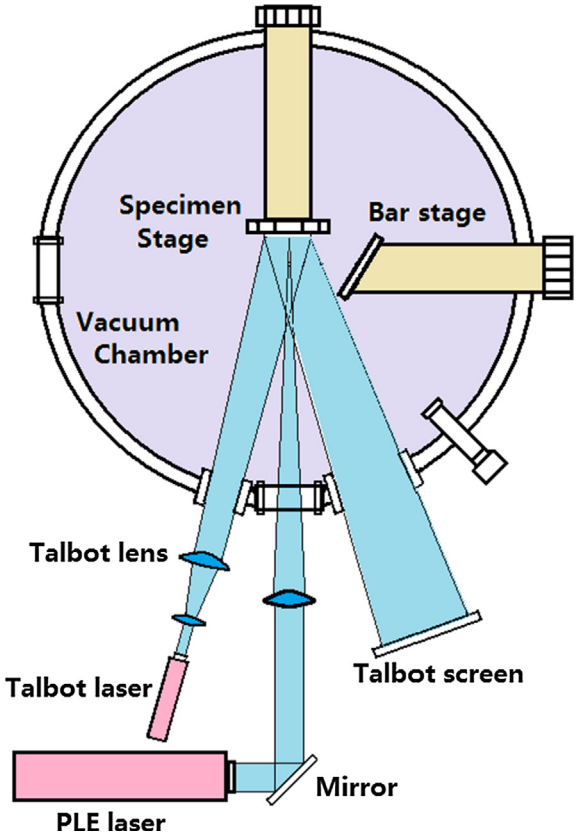


**Fig. 1.** Experimental configuration of the reflecting Talbot image on electron crystal structures observed in PLE process.

$2\pi m)^2$, where $k_f$ is the Fermi vector and q is the quantum number of plasmon, where it is not easy to be excited because of the wider band gap (5–10 eV) [20,21]. While the band gap of low-dimensional plasma becomes narrower or even disappears related to the plasmon term (3/5) $q^2 (hk_f/2\pi m)^2$ in the formula, which is the same as liquid metal which is easy to be excited for emission on surface micro-nanostructures. Here, it is important that the energy distribution of plasmonic emission can exhibit the distribution of the electrons density N on electronic structures.

The plasmonic energy $E_p$ in the surface modes could be given by $E_p = [(hc/2\pi)^2/\varepsilon][(\mathbf{p} - e\mathbf{A})^2 + (m\pi/\Delta)^2]$, where Δ is the surface scale confined, $(\mathbf{p} - e\mathbf{A})$ is the plasmonic momentum [22–24]. The e**A** term of intensive photons plays an important role for generating the electron crystals in no-magnetic field situation on plasma induced by nanosecond pulsed laser. This looks like the Wigner crystals in the strong electric field or the strong magnetic field.

We observe the electron crystal structures by using reflecting Talbot effect. The conventional Talbot effect, discovered in 1836 [25], is well understood by the Fresnel-Kichhoff diffraction theory, as first explained analytically by Lord Rayleigh in 1881 [26], attributing its origin to the interference of diffracted beams. Nowadays, new phenomena and their application, involving reflection Talbot effect image, surface plasmonic structures images and various micro-nanoarrays images, have provided a new way for micro-nanostructures observation and analysis [27–29]. Recently, Zhaoyang Zhang and Min Xiao et al. Experimentally studied the electromagnetically induced Talbot effect in an atomic system [30]. The physical process of reflecting Talbot image could be transformed to a process of transparent Talbot image, equal-effectively, in which just need to change π phase of propagating wave-front. From the Fresnel-Kirchhoff diffraction theory, the diffraction field amplitude A(r) is given by $\Sigma_n A_n \exp[i(\pi\lambda n^2 R_1 r_2)/((R_1 + r_2)d^2)]\exp[-i(2\pi n R_1 r)/((R_1 + r_2) d)]$, in the formula, $R_1$ is the curvature radius of the Gaussian wave-front, $r_2$ is the propagating distance from the reflection object to the observation screen (Talbot screen), and d is the grating constant of periodic structures on sample, where the reflecting Talbot images are localized at $r_2 = r_m \approx m\beta[1 + (m\beta)/R_1]$, in which the m is a grade number of the reflection Talbot image, and the magnifying rate of the reflecting Talbot image is $M_m = 1 + r_m/R_1$. Here, the reflecting Talbot effect with amplification rate of 1000–3000 is used to image on 1D and 2D lattices of electron crystals and plasmons on silicon surface under the illumination of pulsed laser beam.

In our experimental process, a silicon wafer of P-type (1 0 0) oriented substrate with 1–10 Ω cm is taken on the sample stage in the pulsed laser etching (PLE) devices, and a third harmonic of pulsed Nd:YAG laser at 355 nm with nanosecond pulsed width is used to irradiate on Si surface by controlling scanning in vacuum or in oxygen of 100 Pa environment. As shown in Fig. 1, the lattice structure of silicon surface on the specimen stage can be detected on the Talbot screen. In vacuum, the reflecting Talbot magnified images of the electron crystal structures can be observed on silicon surface.

In the reflecting Talbot effect images on silicon, the one-dimensional lattices of electron crystal can be observed on plasma surface induced by nanosecond pulsed laser in vacuum ($10^{-5}$Pa) as shown in Fig. 2(a). And the 2D electron crystal occurs on silicon in vacuum, as shown in the reflecting Talbot effect image of Fig. 2(b), where the transient electron crystal with square lattice is observed. It is interesting that the diffraction pattern of electron crystal lattice with the four-fold symmetry on plasma surface of silicon is exhibited in Fig. 2(c).

It is very interesting that the several electron crystal lattices in the 2D Bravais structures can be observed on plasma surface of silicon by using reflecting Talbot effect images in vacuum. The oblique lattice of transient electron crystal occurs in Fig. 3(a), in which the inset describes its three-fold symmetry. The square lattice of transient electron

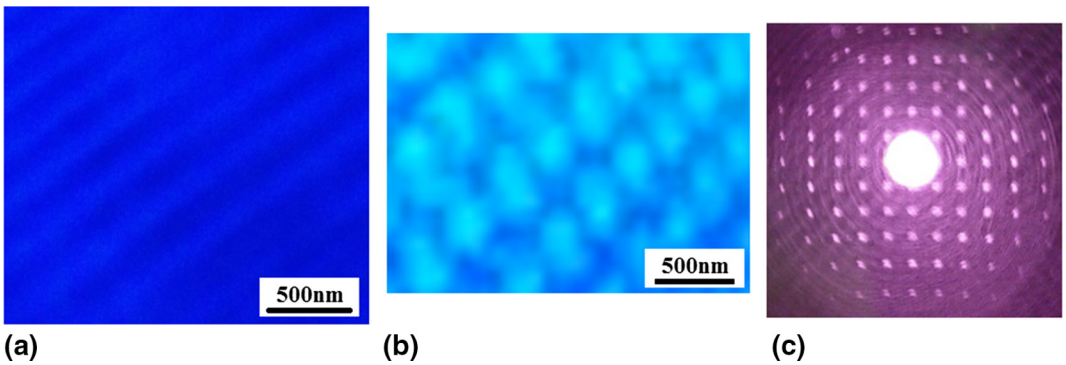


**Fig. 2.** (a) Reflecting Talbot image of the one-dimensional lattices of transient electronic crystal observed on silicon surface plasma in vacuum ($10^{-5}$ Pa); (b) Reflecting Talbot image of the two-dimensional lattices of transient electronic crystal observed on silicon surface plasma in vacuum ($10^{-5}$ Pa); (c) Diffraction pattern of transient electronic crystal with the four-fold symmetry on silicon surface.

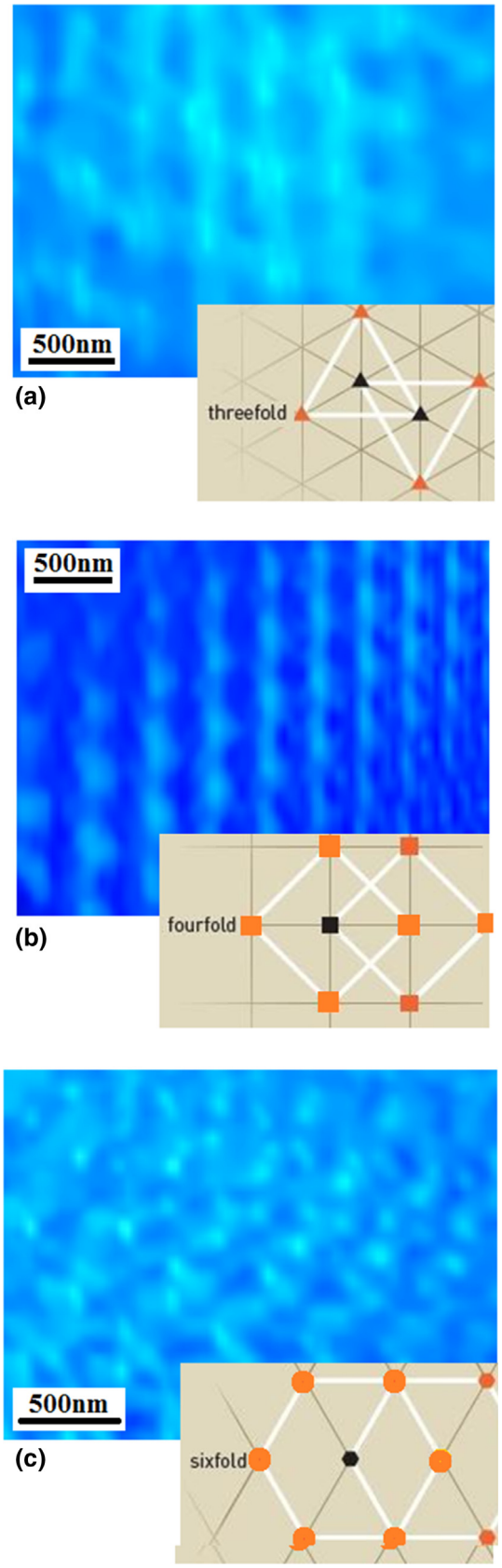


**Fig. 3.** Reflecting Talbot images of transient electronic crystal in the 2D Bravais structures observed on silicon surface in vacuum. (a) Oblique lattice of transient electronic crystal observed, in which the inset describes its three-fold symmetry; (b) Square lattice of transient electronic crystal observed, in which the inset describes its four-fold symmetry; (c) Hexagonal lattice of transient electronic crystal observed, in which the inset describes its six-fold symmetry.

crystal is observed in Fig. 3(b), in which the inset describes its four-fold symmetry. And the hexagonal lattice of transient anomalous electron crystal is observed in the reflecting Talbot effect image of Fig. 3(c), where the inset describes its six-fold symmetry. Here, we can see the various beautiful shapes of the electron crystal structures in the reflecting Talbot effect images. In the experimental observation, it can be guessed that the size of the electron crystal cells is about 100–1 μm.

The lattice points of a 2D Bravais lattice assumed to be in the xy plane, are given by the vectors: $X(l) = l_1 \mathbf{a_1} + l_2 \mathbf{a_2}$, where $\mathbf{a_1}$ and $\mathbf{a_2}$ are the primitive translation vectors of the lattice. And the diffraction points are described by $G(h) = h_1 \mathbf{b_1} + h_2 \mathbf{b_2}$, where $\mathbf{b_1}$ and $\mathbf{b_2}$, which are the primitive translation vectors of the reciprocal lattice. In the 2D Bravais lattices, the structure parameters for the oblique lattice of electron crystal are: $\mathbf{a_1}(a, 0)$, $\mathbf{a_2}(c, b)$, $\mathbf{b_1}(2\pi(1/a, -c/ab))$, $\mathbf{b_2}(2\pi(0, 1/b))$ and $a_c(ab)$; the structure parameters for the square lattice of electron crystal are: $\mathbf{a_1}(a_0, 0)$, $\mathbf{a_2}(0, a_0)$, $\mathbf{b_1}\ (2\pi/\ a_0\ (1, 0))$, $\mathbf{b_2}(2\pi/\ a_0\ (0, 1))$ and $a_c(a_0^2)$; the structure parameters for the hexagonal lattice of electron crystal are: $\mathbf{a_1}(a_0(1, 0))$, $\mathbf{a_2}(a_0(1/2, 3^{1/2}/2))$, $\mathbf{b_1}\ (2\pi/\ a_0\ (1, -3^{1/2}/3))$, $\mathbf{b_2}(2\pi/\ a_0\ (0, 2(3^{1/2}/3)))$ and $a_c((3^{1/2}/2)a_0^2)$. The interaction energy for these lattices of electron crystals can be calculated, in which the interaction energy for the hexagonal lattice of electron crystal is lower, and so it is more stable in the 2D electron crystal structures [31].

Fig. 4 shows the decay spectrum of transient electron crystals on plasma surface, in which the lifetime of the transient electron crystals is about 100 ns. Here, only electron response is faster for forming electron crystal, but it is no way for silicon ions to follow the quickly resonance steps. The faster decay peak on period lattices in vacuum provides an evidence of the electron crystals.

It is interesting to make comparison between the electron crystal lattices occurring in vacuum and the plasmonic lattice occurring in oxygen with 100 Pa environment. Fig. 5(a) shows the reflecting Talbot image of the plasmonic lattice with silicon ions on surface in oxygen with 100 Pa, which relates to the slower decay peak with lifetime of 10 μs in decay spectrum, as shown in Fig. 5(b).

Under nanosecond pulsed laser irradiation on silicon surface, the interaction between photons and plasmons produces surface electron gas on silicon ions background in vacuum, where photons resonance with high frequency quickly carries with electrons in plasma to generate the electron crystal on surface. Here, only electrons can follow with the photons resonance with high frequency to separate the electrons from plasma for generating electron crystals on surface, whose principle diagram is shown in Fig. 6.

After condensing, the N type region can be built in top silicon layer by electrons injection on surface, and the P type region can be formed in bottom silicon layer by ions injection on background, as shown in Fig. 7(a). We can fabricate the PN junction structure and the photovoltaic system by using nanosecond pulsed laser on pure silicon chip in vacuum, on which the I-V curves with PN junction characteristic are measured. In Fig. 7(b), the black curve shows the I-V evolution in dark field, and the blue curve exhibits the I-V evolution in light field of xenon lamp on the PN junction sample prepared in vacuum.

In conclusion, we have studied 2D transient electron crystals on plasma surface in no-magnetic field situation, which is similar with the Wigner crystal structure. It is demonstrated that the electron crystal can be built on silicon surface in an intensive photonic field, as well as doing that in strong electric field and strong magnetic field. In the experimental investigation, the lattice structures of transient electron crystals were observed during nanosecond pulsed laser interaction on silicon surface in vacuum, by using reflecting Talbot effect images, where the oblique lattice, the square lattice and the hexagonal lattice were measured in the 2D Bravais lattices of the transient electron crystal with photons resonance. The faster decay peak with lifetime of 100 ns measured provides evidence of the transient electron crystals occurring in vacuum. These new phenomena will have a good application in the quantum photo-electronic devices. Under irradiation of the nanosecond pulsed laser on silicon surface, the interaction between

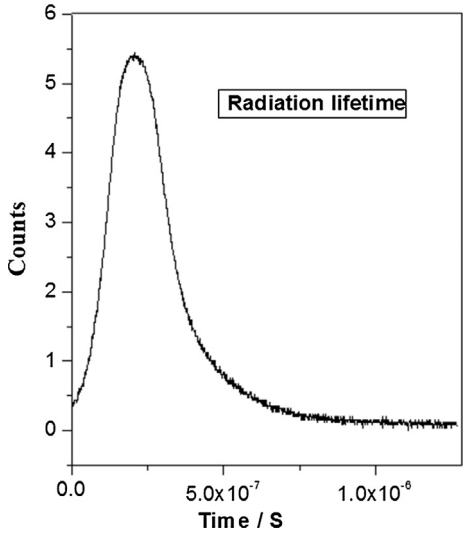


**Fig. 4.** Decay spectrum of transient electronic crystals, in which its lifetime is about 100 ns.

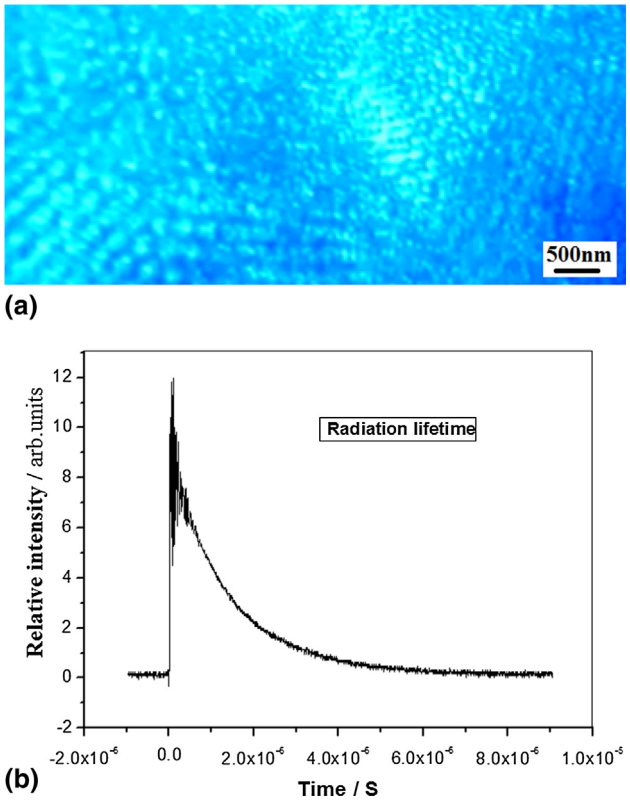


**Fig. 5.** (a) Reflecting Talbot image of plasmonic lattice occurring on silicon surface in oxygen with 100 Pa environment; (b) Decay spectrum of lattices emission, in which the plasmonic lattice with silicon ions relates to the slower decay peak with lifetime of 10 μs.

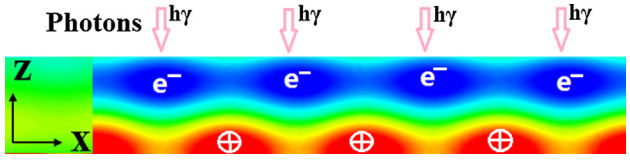


**Fig. 6.** Separation structure of electrons and silicon ions in plasma under photonic resonance, in which electrons float on surface to form surface electrons gas on silicon ions background.

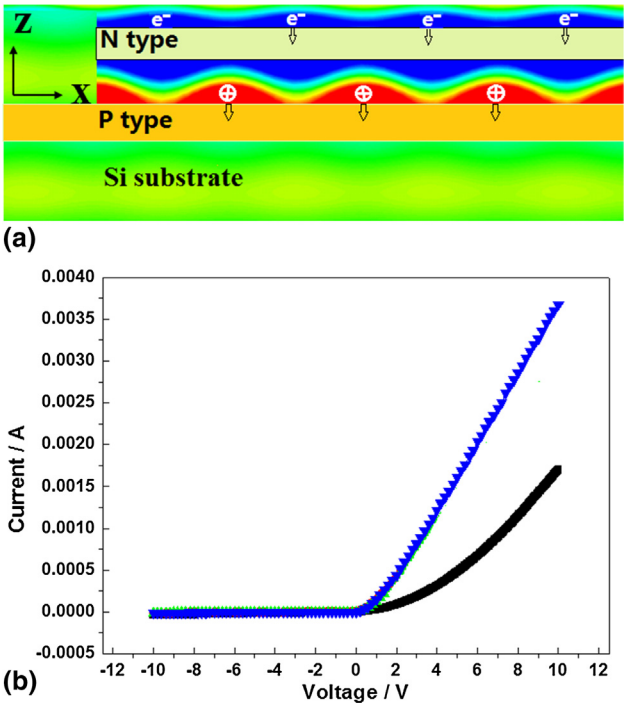


**Fig. 7.** (a) Injection schematic diagram for forming PN junction with defects, in which the N type region can be formed in top silicon layer through electrons injection on surface, and the P type region can be formed in bottom silicon layer through ions injection on background; (b) I-V curves measured on the PN junction structure and the photo-voltaic system prepared by using nanosecond pulsed laser on pure silicon chip in vacuum($10^{-5}$ Pa), in which the black curve shows the I-V evolution in dark field, and the blue curve exhibits the I-V evolution in light field of xenon lamp. (For interpretation of the references to colour in this figure legend, the reader is referred to the web version of this article.)

photons and plasmons produces surface electron gas on silicon ions background in vacuum. Here, a new way for building PN junction by photons in vacuum will be developed.

## Acknowledgements

This work was supported by the National Natural Science Foundation of China (Grant No. 61465003).

## References

[1] E.P. Wigner, Phys. Rev. 46 (1934) 1002.
[2] E.P. Wigner, Trans. Faraday Soc. 34 (1938) 678.
[3] F.W. de Wette, Phys. Rev. A 135 (1964) 287.
[4] R.S. Crandall, R.W. Williams, Phys. Lett. A 34 (7) (1971) 404.
[5] A.V. Chaplik, Sov. Phys. -JETP 35 (1972) 395.
[6] P.M. Platzman, H. Fukuyama, Phys. Rev. B 10 (1974) 3150.
[7] F. Stern, Phys. Rev. Lett. 18 (1967) 546.
[8] K.W. Chiu, J.J. Quinn, Rev. B 9 (1974) 4724.
[9] H.A. Fertig, Phys. Rev. B 59 (1999) 2120.
[10] M.M. Fogler, D.A. Huse, Phys. Rev. B 62 (2000) 7553.
[11] A.I. Larkin, Sov. Phys. JETP 31 (1970) 784.
[12] A.I. Larkin, Y.N. Ovchinnikov, J. Low Temp. Phys. 34 (1979) 409.
[13] P.D. Ye, L.W. Engel, D.C. Tsui, R.M. Lewis, L.N. Pfeiffer, K. West, Phys. Rev. Lett. 89 (2002) 176802.
[14] Chi Zhang, M. Rui-Rui Du, J. Manfra, L.N. Pfeiffer, K.W. West, Phys. Rev. B 92 (2015) 075434.
[15] Joonho Jang, Benjamin M. Hunt, Loren N. Pfeiffer, Nat. Phys. 10 (2016) 1038.
[16] Yanpeng Zhang, Zhiguo Wang, Zhiqiang Nie, Changbiao Li, Haixia Chen, Lu. Keqing, Min Xiao, Phys. Rev. Lett. 106 (2011) 093904.
[17] Yiqi Zhang, Wu Zhenkun, Milivoj R. Belíc, Huaibin Zheng, Zhiguo Wang, Min Xiao, Yanpeng Zhang, Laser Photonics Rev. 9 (2015) 331.
[18] Zhaoyang Zhang, Yiqi Zhang, Jiteng Sheng, Liu Yang, Mohammad-Ali Miri, Demetrios N. Christodoulides, Bing He, Yanpeng Zhang, Min Xiao, Phys. Rev. Lett. 117 (2016) 123601.

[19] W.Q. Huang, L. Xu, K.Y. Wu, S.R. Liu, J. Appl. Phys. 102 (2007) 053517.
[20] D. Englund, D. Fattal, E. Waks, G. Solomon, B. Zhang, T. Nakaoka, Y. Arakawa, Y. Yamamoto, Phys. Rev. Lett. 95 (2005) 013904.
[21] L.L. Li, W. Xu, Appl. Phys. Lett. 104 (2014) 111603.
[22] R. Lo Savio, S.L. Portalupi, D. Gerace, A. Shakoor, T.F. Kruass, L. O'Faolain, L.C. Andreani, M. Galli, Appl. Phys. Lett. 98 (2011) 201106.
[23] C. Chang-Hee, O.A. Carlos, P. Joohee, A. Ritesh, Nat. Photon. 7 (2013) 285.
[24] C.H. Cho, C.O. Aspetti, M.E. Turk, J.M. Kikkawa, S.W. Nam, R. Agarwal, Nat. Mater. 10 (2011) 669.
[25] H.F. Talbot, Philos. Mag. 9 (1836) 401.
[26] L. Rayleigh, Philos. Mag. 11 (1881) 196.
[27] Y. Zhang, J.M. Wen, S.N. Zhu, et al., Phys. Rev. Lett. 104 (2010) 183901.
[28] W.I. Li, H.Y. Li, B. Gao, Y.T. Yu, Sci. Rep. 7 (2017) 45573.
[29] K. Li, F. Xia, M. Wang, P. Sun, T.T. Liu, W.P. Hu, W. Kong, M.J. Yun, L.F. Dong, Carbon 118 (2017) 192–199.
[30] Zhaoyang Zhang, Xing Liu, Dan Zhang, Jiteng Sheng, Yiqi Zhang, Yanpeng Zhang, Min Xiao, Phys. Rev. A 97 (2018) 013603.
[31] Lynn Bonsall, A.A. Maradudin, Phys. Rev. B 15 (1977) 1959.